

UNMASKING TREES FOR TABULAR DATA

Anonymous authors

Paper under double-blind review

ABSTRACT

Despite much work on advanced deep learning and generative modeling techniques for tabular data generation and imputation, traditional methods have continued to win on imputation benchmarks. We herein present UnmaskingTrees, a simple method for tabular imputation (and generation) employing gradient-boosted decision trees which are used to incrementally unmask individual features. This approach offers state-of-the-art performance on imputation, and on generation given training data with missingness; and it has competitive performance on vanilla generation. To solve the conditional generation subproblem, we propose a tabular probabilistic prediction method, BaltoBot, which fits a *balanced tree of boosted tree classifiers*. Unlike older methods, it requires no parametric assumption on the conditional distribution, accommodating features with multimodal distributions; unlike newer diffusion methods, it offers fast sampling, closed-form density estimation, and flexible handling of discrete variables. We finally consider our two approaches as meta-algorithms, demonstrating in-context learning-based generative modeling with TabPFN.

1 INTRODUCTION

Given a tabular dataset, it is frequently desirable to impute missing values within that dataset, and to generate new synthetic examples. On data generation, recent work (Jolicoeur-Martineau et al., 2024b) (ForestDiffusion) has shown state-of-the-art results on data generation using gradient-boosted trees (Chen & Guestrin, 2016) trained on diffusion or flow-matching objectives, outperforming deep learning-based approaches. However, this approach tended to struggle on tabular imputation tasks, outperformed by MissForest (Stekhoven & Bühlmann, 2012), an older multiple imputation approach based on random forests (Breiman, 2001).

We address this shortfall by training gradient-boosted trees to autoregressively unmask features in random order, via permutation language modeling (Yang, 2019). This autoregressive approach, which we dub UnmaskingTrees, naturally performs conditional generation (i.e. imputation): we simply fill in and condition on observed values, autoregressively generating the remaining missing values. This contrasts with tabular diffusion modeling, for which the RePaint inpainting algorithm (Lugmayr et al., 2022) is employed to mediocre effect (Jolicoeur-Martineau et al., 2024b). Because the predictor for a given feature must condition on varying subsets of the other features, the ability of gradient-boosted trees to handle missing features makes them a natural choice for autoregressive modeling. Hence, we maintain the tree-based approach of Jolicoeur-Martineau et al. (2024b), while replacing their tree-based regressors with our novel tree-based probabilistic predictors, which we turn to next.

While mean-estimating regression models are satisfactory for diffusion, for autoregression we must inject noise, and hence must estimate the entire conditional distribution of each feature. We therefore revisit the long-studied problem of (tabular) probabilistic prediction (Le et al., 2005; Meinshausen & Ridgeway, 2006). Because the conditional distribution is possibly multi-modal, parametric approaches such as XGBoostLSS (März, 2019), NGBoost (Duan et al., 2020), and PGBM (Sprangers et al., 2021) are poor choices for our setting. Meanwhile, quantization of a continuous variable can model its multi-modality, but at the cost of destroying either low-resolution or high-resolution information. A diffusion-based method, Treeffuser Beltran-Velez et al. (2024), was recently proposed to address these problems. However, as a diffusion method, it suffers from slow sampling and is unable to provide closed-form density estimates; furthermore, Treeffuser does not naturally model discrete outcomes. To address these problems, we propose BaltoBot, a *balanced tree of boosted trees*. For each individual variable, we recursively divide its output space with the kernel density integral (KDI)

054 quantizer (McCarter, 2023) into a “meta-tree” of binary classifiers, which for us are gradient-boosted
 055 trees. This allows us to efficiently generate samples and estimate densities, because each sample
 056 follows only one path from root to leaf of the meta-tree. Performing regression with hierarchical
 057 classification proved successful in computer vision object bounding box prediction (Li et al., 2020),
 058 but has been surprisingly underexplored in tabular ML and in generative modeling.

059 Our two methods are in fact meta-algorithms that, in combination, can create a generative model out
 060 of *any* probabilistic binary classifier. To demonstrate this flexibility, we swap out XGBoost (Chen &
 061 Guestrin, 2016) for TabPFN (Hollmann et al., 2022). TabPFN is a deep learning model pretrained
 062 to perform in-context learning for tabular classification. While it has state-of-the-art classification
 063 benchmark performance (McElfresh et al., 2024), it currently does not perform regression tasks, nor
 064 does it inherently perform generative modeling (Ma et al., 2024). Constructing a generative model
 065 out of TabPFN (Hollmann et al., 2022) was first proposed in TabPFGen (Ma et al., 2024), which
 066 approximates the posterior from TabPFN-provided likelihoods by iteratively applying stochastic
 067 gradient Langevin dynamics (Welling & Teh, 2011). But unlike the previous work, ours requires only
 068 a few TabPFN forward-passes for each sample rather than many iterative data updates.

069 We showcase UnmaskingTrees on two tabular case studies, and on the benchmark of 27 tabular
 070 datasets presented by Jolicoeur-Martineau et al. (2024b). Most notably on this benchmark, our
 071 approach offers state-of-the-art performance on imputation and on generation given training data
 072 with missingness; and it has competitive performance on vanilla generation. We also demonstrate
 073 that BaltoBot is on its own a promising method for probabilistic prediction, showing its advantages
 074 on synthetic case studies and on a heavy-tailed sales forecasting benchmark.

075 Finally, we provide code with an easy-to-use sklearn-style API at [https://github.com/
 076 another-anonymous-account/unmasking-trees](https://github.com/another-anonymous-account/unmasking-trees). In addition to being useful for practi-
 077 tioners, we hope our work sparks study within the tabular ML community about whether diffusion or
 078 autoregression is better for tabular data. [Previous autoregressive tabular modeling methods, TabMT
 079 \(Gulati & Roysdon, 2024\) and DP-TBART \(Castellon et al., 2023\), use Transformer \(Vaswani, 2017\)
 080 models, making them less applicable for the GPU-poor.](#) Our simple, efficient implementations of
 081 UnmaskingTrees and BaltoBot contribute to investigating this question.

083 2 METHOD

085 2.1 UNMASKINGTREES FOR TABULAR JOINT DISTRIBUTION MODELING

087 UnmaskingTrees combines the gradient-boosted trees of ForestDiffusion (Jolicoeur-Martineau et al.,
 088 2024b) with the training objective of generalized autoregressive language modeling (Yang, 2019),
 089 inheriting the benefits of both. Consider a dataset with N examples and D features. [We learn the
 090 joint distribution over \$D\$ -dimensional example \$\mathbf{x}\$ by maximizing the expected log-likelihood with
 091 respect to all possible permutations of the factorization order,](#)

$$093 \log p(\mathbf{x}) = \log \mathbb{E}_{\sigma \in \mathcal{U}(G_D)} \left[\prod_{t=1}^D p(x_{\sigma(t)} | \mathbf{x}_{\sigma(<t)}) \right],$$

096 where σ is a permutation drawn uniformly from $\mathcal{U}(G_D)$, the permutation group on D features; $\mathbf{x}_{\sigma(<t)}$
 097 denotes all features that precede the t -th feature in the permuted sequence of features. If we were
 098 to have marginalized over permutations, we would have obtained a masked language modeling
 099 procedure with a randomly-sampled masking rate $r \sim \mathcal{U}(0, 1)$ (Kitouni et al., 2023; 2024); such a
 100 procedure was previously shown to have benefits in combination with tabular Transformer models
 101 (Gulati & Roysdon, 2024) (TabMT).

102 For each example, we generate new training samples by randomly sampling an order over the features,
 103 then incrementally masking the features in that random order. Given duplication factor K , we repeat
 104 this process K times with K different random permutations, leading to a training dataset with KND
 105 samples. Given this, we train XGBoost (Chen & Guestrin, 2016) models to predict each unmasked
 106 sample given the more-masked example derived from it, one per feature. [We model categorical
 107 features via softmax-based classification with cross-entropy loss; our approach for continuous features
 is described in Section 2.2.](#)

For both generation and imputation, we generate features of each sample in random order. For imputation rather than generation tasks, we begin by filling in each sample with the observed values, and run inference on the remaining unobserved features. Implementing this is very simple: it requires about 70 lines of Python code for training, and about 20 lines for inference.

2.2 BALTOBOT FOR TABULAR PROBABILISTIC PREDICTION

A key problem when autoregressively generating continuous data is that a regression model will attempt to predict the mean of a conditional distribution, whereas we would like it to sample from the possibly-multimodal conditional distribution. The simplest solution is to quantize continuous features into bins, because classification over histograms is inherently multimodal; TabMT (Gulati & Roysdon, 2024) did this with 1d k-Means clustering (Lloyd, 1982). Yet this not only destroys information within bins due to rounding, it also destroys information about the proximity among the ordered bins. Thus, it forces us to choose between a small number of quantization bins, yielding low resolution; or to choose a large number of bins, risking catastrophic errors due to overfitting and/or clumping of generated samples due to poor calibration. This not only limits performance, but also necessitates hyperparameter tuning (Gulati & Roysdon, 2024).

Inspired by this, we propose a general-purpose solution to the tabular probabilistic prediction problem. For each individual regression output variable, we build a **height- H** balanced tree of binary classifiers. Consider a **node with height h** on this “meta-tree”, which is fit with $(\mathbf{X}_{\text{train}} \in \mathbb{R}^{n \times d}, \mathbf{y}_{\text{train}} \in \mathbb{R}^n)$. Using kernel density integral quantization (KDI) (McCarter, 2023), which adaptively interpolates between uniform quantization and quantile quantization, we obtain binarized $\tilde{\mathbf{y}}_{\text{train}} \in [0, 1]^n$. **Thus, the input space to every node is partitioned into two with the splitting point determined by KDI.** We train an XGBoost classifier on $(\mathbf{X}_{\text{train}}, \tilde{\mathbf{y}}_{\text{train}})$. If $h > 0$, we then recursively pass $\{(\mathbf{X}^{(i)}, y^{(i)}) \in (\mathbf{X}_{\text{train}}, \mathbf{y}_{\text{train}}) | \tilde{y}^{(i)} = 0\}$ to its left child, and analogously for $\tilde{y}^{(i)} = 1$ to its right child. At a leaf node, $h = 0$, if given a single unique training set output value in a bin, we record this value. At inference time, given a query input \mathbf{X} , we descend the tree by obtaining predicted probabilities from each node’s XGBoost classifier, then sampling from these. Once we reach a leaf node, we either sample uniformly from its appropriate bin, or we return the lone output value if a singleton bin.

At training and inference time, each XGBoost model within the meta-tree only sees examples that fall into its corresponding region of the output space. Thus, for a meta-tree with height H (and thus 2^H models), each example is only passed as input to H different models. While lower-level classifiers receive less data and are poorer quality, the magnitude of such errors are smaller due to our hierarchical partitioning approach. Furthermore, our singleton-bin technique allows us to adaptively generate discrete and even mixed-type variables, if these discrete outcomes are high-frequency relative to the total size of the data and to the height of the meta-tree. (Up to 2^H discrete outcomes can be produced by BaltoBot.) Finally, eschewing diffusion modeling enables us to perform closed-form conditional density estimation.

[Algorithms for UnmaskingTrees and BaltoBot are given in Appendix Section A.](#)

2.3 COMPUTATIONAL COMPLEXITY

ForestDiffusion, with T diffusion steps and duplication factor K , constructs a training dataset of size $TKN \times D$. Given the same duplication factor K , UnmaskingTrees will construct a training dataset of size $KND \times D$. Meanwhile, ForestDiffusion must train DT different XGBoost regression models. We, on the other hand, train D different BaltoBot models, one per feature; with BaltoBot meta-tree height of H , we then train a total of $D2^H$ XGBoost binary classifiers. However, classifiers lower in the BaltoBot meta-tree become progressively faster to train. Indeed, each constructed training sample will be seen by DT different XGBoost regressors with ForestDiffusion, but only DH classifiers with our approach. Given that $T \sim 50$ and $H \sim 4$, this yields a large speedup for our approach.

The KDI quantizer (McCarter, 2023) has negligible contribution to runtime, because it uses the polynomial-exponential kernel density estimator (KDE) (Hofmeyr, 2019), which has linear complexity in sample size for 1d data, unlike the quadratic complexity of the Gaussian KDE.

At inference time, each ForestDiffusion generated sample passes through T steps of the diffusion reverse-process, for a total of DT XGBoost predictions. For UnmaskingTrees with BaltoBot, each generated sample instead requires only DH XGBoost predictions, because each sample follows only

one path from root to leaf of the meta-tree. The resulting speedup is especially impactful for the multiple imputation scenario, where inference time dominates.

2.4 IN-CONTEXT LEARNING-BASED GENERATION WITH BALTOBOTABPFN AND UNMASKINGTABPFN

Within our flexible frameworks for joint and conditional modeling, TabPFN (Hollmann et al., 2022) can be used as a base learner for probabilistic prediction and generative modeling. For UnmaskingTabPFN joint modeling, a difficulty arises from TabPFN’s inability to handle inputs $\mathbf{X}_{\text{train}}$ with missing values (NaNs). To address this, we developed NanTabPFN, a wrapper for TabPFN that supports missingness in both training and test features. Based on each test query \mathbf{x}_{test} , we select row indices \mathcal{R} and column indices \mathcal{C} so that $[\mathbf{X}_{\text{train}}]_{\mathcal{R},\mathcal{C}}$ has no NaNs, using the following key idea. Consider a particular train example $\mathbf{x}_{\text{train}}$ and test query \mathbf{x}_{test} , with visible (non-missing) features denoted by sets $\mathcal{V}(\mathbf{x}_{\text{train}})$ and $\mathcal{V}(\mathbf{x}_{\text{test}})$. We can maximize the number of utilized features, while also ensuring that TabPFN receives no NaNs, by restricting the set of columns to those observed for the test query, $\mathcal{C} := \mathcal{V}(\mathbf{x}_{\text{test}})$, then choosing training examples $\mathcal{R} := \{i | \mathcal{C} \subseteq \mathcal{V}(\mathbf{x}_{\text{train}}^{(i)})\}$. In practice, our procedure is more complicated, because the above choices may result in either empty \mathcal{C} or empty \mathcal{R} . If \mathcal{R} is empty, we incrementally set random features of \mathbf{x}_{test} to missing until we are able to obtain a non-empty training set. If \mathcal{C} is empty, we introduce a new all-1s feature to both $\mathbf{X}_{\text{train}}$ and \mathbf{x}_{test} .

3 RESULTS

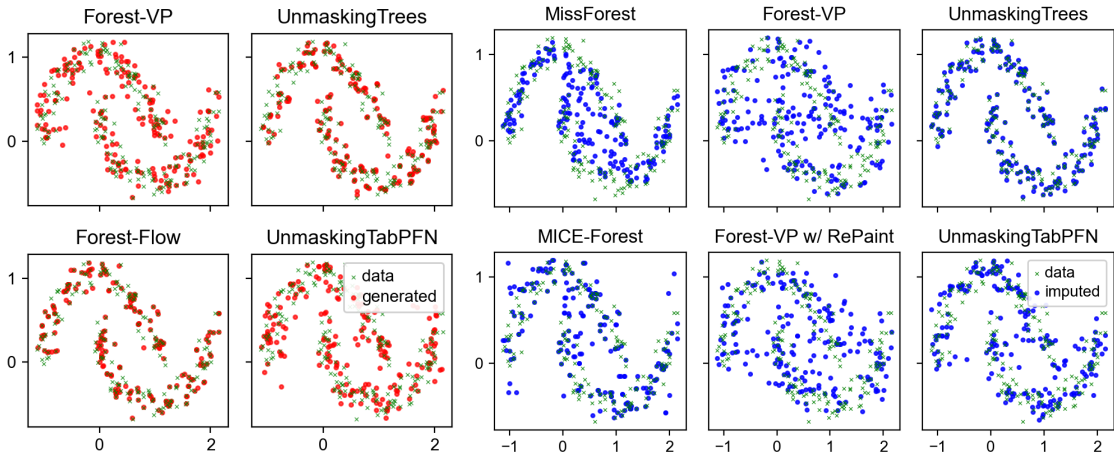


Figure 1: Results on Two Moons case study. Original data is shown in green; generated data is shown in red; imputed data is shown in blue.

We evaluate UnmaskingTrees on two case studies (Section 3.1) and on a tabular benchmark of 27 datasets (Section 3.2). We then evaluate BaltoBot and BaltoBoTabPFN on tabular probabilistic prediction case studies (Section 3.3) and on a sales forecasting dataset (Section 3.4). Results were obtained always using the default hyperparameters: output tree height of 4, and duplication factor $K = 50$. These hyperparameter values were tuned on the Two Moons and Iris case studies, then applied without further tuning to the remaining experiments, because hyperparameter tuning is no fun at all. XGBoost hyperparameters were set to their defaults. Experiments were performed on a iMac (21.5-inch, Late 2015) with 2.8GHz Intel Core i5 processor and 16GB memory.

Overall, UnmaskingTrees (using BaltoBot) has state-of-the-art performance on imputation and on generation after training on incomplete data; and it has competitive performance on vanilla tabular generation scenarios. We further demonstrate the benefits of BaltoBot and BaltoBoTabPFN when evaluated in their own right for probabilistic prediction.

216
217
218
219
220
221
222
223
224
225
226
227
228
229
230
231
232
233
234
235
236
237
238
239
240
241
242
243
244
245
246
247
248
249
250
251
252
253
254
255
256
257
258
259
260
261
262
263
264
265
266
267
268
269

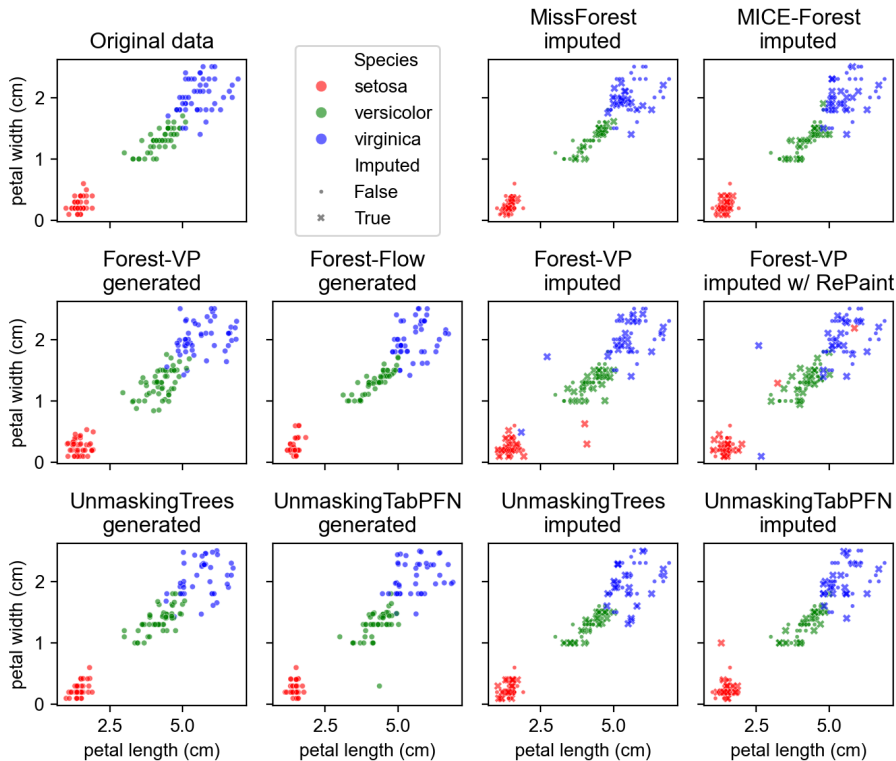


Figure 2: Results on Iris dataset, with species, petal width, and petal length depicted. Original data and synthetically-generated datasets are shown on the left columns. The imputed dataset is shown on the right columns, with \times symbols highlighting the samples with any missingness that required imputation.

3.1 CASE STUDIES ON TWO MOONS AND IRIS DATASETS

Two Moons dataset We first compare our approach to previous leading methods on the synthetic Two Moons dataset with 200 training samples and noise level $\mathcal{N}(0, 0.1)$. We compare UnmaskingTrees to MissForest (Stekhoven & Bühlmann, 2012), MICE-Forest (Van Buuren et al., 1999; Wilson et al., 2022) (another popular traditional multiple imputation method), and ForestDiffusion, with default hyperparameters for all methods. For ForestDiffusion, we evaluate both the variance-preserving SDE diffusion (Forest-VP) and flow-matching (Forest-Flow) versions on generation; on imputation, we evaluate Forest-VP with and without RePaint, again using default RePaint hyperparameters; Forest-Flow does not support imputation.

We show results in Figure 1. On generation, Forest-VP appears to do best according to visual inspection, while UnmaskingTrees and Forest-Flow perform similarly decently. UnmaskingTabPFN performs poorly, but does capture the overall shape of the distribution. Next, we turn to imputation, wherein we request a single imputation for a copy of the original training data with the second dimension (y -axis) values masked out. ForestDiffusion struggles with and without RePaint, with substantial out-of-distribution imputations, and MissForest and MICE-Forest share this problem to lesser degrees. Meanwhile, UnmaskingTrees generates impeccable imputations.

Iris dataset In Figure 2, we show results for the Iris dataset (Fisher, 1936), plotting petal length, petal width, and species. We compare both methods on generation, and to compare on imputation, we create another version of the Iris dataset, with missingness completely at random: we randomly select samples with 50% chance to have any missingness, and on these samples, we mask the non-species feature values with 50% chance. Visually, ForestDiffusion and UnmaskingTrees perform about equally well on generation. Meanwhile, on imputation, UnmaskingTrees does a better job

conditioning on species information than ForestDiffusion. UnmaskingTrees also produces more diverse imputations than MissForest.

3.2 BENCHMARKING UNMASKINGTREES ON 27 TABULAR DATASETS

Imputation Here, we add UnmaskingTrees to the benchmark of 8 imputation methods on 27 public datasets, evaluated according to 9 metrics, developed by Jolicoeur-Martineau et al. (2024b) for evaluating tabular imputation and generation methods. **This benchmark primarily contains smaller-sized (with $103 \leq N \leq 20,640$ and $4 \leq D \leq 90$) datasets, which our approach is especially geared towards.** Namely, we compare our approach against Forest-VP Jolicoeur-Martineau et al. (2024b), as well as k-NN imputation (Troyanskaya et al., 2001), ICE (Buck, 1960), MICE-Forest (Van Buuren et al., 1999; Wilson et al., 2022), MissForest (Stekhoven & Bühlmann, 2012), Softimpute (Hastie et al., 2015), minibatch Sinkhorn optimal transport (Muzellec et al., 2020), and generative adversarial nets (GAIN) (Yoon et al., 2018).¹ We follow Jolicoeur-Martineau et al. (2024b) in computing the per-dataset rank of each method relative to other methods, then reporting the average over 27 datasets. For all methods other than our own, we compute ranks by reusing the raw scores provided in Jolicoeur-Martineau et al. (2024b)’s code repository.

Results for imputation are shown in Table 1. UnmaskingTrees wins first place on 3/9 metrics, including both metrics based on downstream prediction tasks; and it generally outperforms ForestDiffusion, winning on 8/9 metrics. While MissForest wins first place on 4/9 metrics, UnmaskingTrees wins 5-4 head-to-head vs MissForest; UnmaskingTrees has average *averaged rank* of 3.2 compared to 3.5 for MissForest. UnmaskingTrees is also the only method with better than 5th place rank on all metrics.

We report further ablation experiments in Table 2, wherein we run UnmaskingTrees without BaltoBot, and instead with vanilla quantization using k-Means clustering (Lloyd, 1982) and KDI quantization (McCarter, 2023). Results showing progressive improvements for the UnmaskingTrees framework, for KDI quantization versus k-Means, and for the BaltoBot method used in our full proposed solution.

Table 1: Tabular data imputation (27 datasets, 3 experiments per dataset, 10 imputations per experiment) with 20% missing. Shown are *averaged rank* over all datasets and experiments (standard-error). Overall best is **highlighted**; better of Forest-VP versus ours is **boldface blue**. Metrics are Minimum and Average mean-absolute error (MinMAE and AvgMAE) to ground-truth, Wasserstein distance to train and test dataset distributions (W_{train} and W_{test}), Mean Absolute Deviation (MAD) around the median/mode (for diversity), R^2 and F_1 for downstream regression / classification problems, and percent bias P_{bias} and confidence interval coverage rate Cov_{rate} for statistical inferences.

	MinMAE ↓	AvgMAE ↓	W_{train} ↓	W_{test} ↓	MAD ↓	R^2 ↓	F_1 ↓	P_{bias} ↓	Cov_{rate} ↓
KNN	5.5 (0.5)	6.3 (0.4)	4.9 (0.4)	5.0 (0.4)	8.4 (0)	6.5 (1)	5.7 (1.1)	6.2 (1)	5.4 (0.6)
ICE	6.8 (0.4)	4.7 (0.4)	7.0 (0.5)	7.2 (0.4)	1.6 (0.2)	6.2 (1)	7.0 (0.6)	5.7 (0.9)	5.3 (0.6)
MICE-Forest	3.9 (0.4)	2.5 (0.4)	2.9 (0.2)	3.0 (0.2)	3.6 (0.2)	3.7 (1.4)	3.2 (1)	5.5 (1.2)	4.3 (0.6)
MissForest	2.7 (0.5)	4.0 (0.4)	1.8 (0.3)	2.0 (0.3)	5.5 (0.2)	3.8 (1.4)	2.5 (0.5)	5.5 (1.5)	3.3 (0.5)
Softimpute	6.7 (0.4)	7.6 (0.4)	7.1 (0.5)	7.3 (0.5)	8.4 (0)	6.0 (0.9)	7.8 (0.4)	6.3 (0.9)	6.7 (0.4)
OT	5.9 (0.4)	6.1 (0.3)	6.0 (0.5)	6.0 (0.5)	3.7 (0.3)	6.2 (0.5)	6.8 (0.6)	5.5 (0.8)	4.8 (0.5)
GAIN	4.7 (0.4)	6.5 (0.3)	6.0 (0.3)	6.0 (0.2)	6.9 (0.1)	5.7 (0.8)	5.4 (0.8)	4.7 (1)	5.0 (0.6)
Forest-VP	5.3 (0.4)	4.0 (0.5)	5.8 (0.3)	5.1 (0.4)	3.2 (0.4)	4.5 (0.9)	4.6 (0.8)	3.3 (0.6)	5.5 (0.7)
UTrees	3.5 (0.5)	3.2 (0.5)	3.5 (0.4)	3.5 (0.5)	3.8 (0.2)	2.5 (0.6)	2.2 (0.6)	2.3 (0.9)	4.7 (0.6)

Generation with and without missingness We next repeat the experimental setup of Jolicoeur-Martineau et al. (2024b) for evaluating tabular generation methods. For tabular generation, using the same 27 datasets, Jolicoeur-Martineau et al. (2024b) benchmark their methods (Forest-VP and Forest-Flow) against 6 other methods, namely, Gaussian Copula (Joe, 2014), tabular variational autoencoding (TVAE) (Xu et al., 2019), two conditional generative adversarial net methods (CTGAN (Xu et al., 2019) and CTAB-GAN+ (Zhao et al., 2021)), and two other tabular diffusion methods (STaSy (Kim et al., 2022) and TabDDPM (Kotelnikov et al., 2023)). These are evaluated with 9 metrics, in the vanilla fully-observed setting and in the synthetically-induced 20% missing completely at random (MCAR) setting.

Results for partially-missing data are shown in Table 3. UnmaskingTrees is first place on 5/9 metrics; head-to-head, UnmaskingTrees beats TabDDPM 5-4, and beats Forest-Flow 6-3. Results for fully-

¹We do not add TabMT (Gulati & Roysdon, 2024) and TabPFGen (Ma et al., 2024) to the benchmark because no code was provided. We do not add UnmaskingTabPFN because of out-of-memory errors on our machine.

Table 2: Averaged ranks from ablation study of tabular data imputation (27 datasets, 3 experiments per dataset, 10 imputations per experiment) with 20% missing. Shown are *averaged rank* over all datasets and experiments (standard-error). Overall best is **highlighted**; better of Forest-VP versus ours is **boldface blue**. See Table 1 for column meanings.

	MinMAE ↓	AvgMAE ↓	W_{train} ↓	W_{test} ↓	MAD ↓	R^2 ↓	F_1 ↓	P_{bias} ↓	Cov_{rate} ↓
KNN	6.8 (0.6)	7.8 (0.6)	6.0 (0.4)	6.1 (0.5)	10.4 (0)	8.2 (1.3)	7.0 (1.5)	7.5 (1.5)	6.5 (0.8)
ICE	8.3 (0.5)	5.8 (0.5)	8.5 (0.6)	8.8 (0.5)	1.9 (0.4)	8.0 (1.1)	9.0 (0.6)	7.2 (1.1)	6.4 (0.8)
MICE-Forest	4.8 (0.6)	3.3 (0.6)	3.5 (0.3)	3.4 (0.3)	4.6 (0.4)	4.3 (1.8)	4.3 (1.3)	6.8 (1.6)	4.8 (0.7)
MissForest	3.3 (0.7)	5.0 (0.6)	2.2 (0.4)	2.3 (0.4)	7.2 (0.3)	4.7 (1.8)	3.3 (0.9)	6.8 (1.9)	3.8 (0.6)
Softimpute	8.3 (0.5)	9.3 (0.5)	8.8 (0.6)	8.9 (0.6)	10.4 (0)	7.5 (1.2)	9.8 (0.4)	8.3 (0.9)	7.9 (0.6)
OT	7.2 (0.5)	7.6 (0.4)	7.4 (0.6)	7.4 (0.6)	4.8 (0.4)	8.2 (0.5)	8.8 (0.6)	7.3 (0.7)	5.8 (0.7)
GAIN	5.8 (0.5)	8.3 (0.4)	7.2 (0.5)	7.5 (0.4)	8.9 (0.1)	7.5 (0.8)	7.4 (0.8)	6.7 (1)	6.1 (0.8)
Forest-VP	6.4 (0.5)	4.8 (0.6)	7.0 (0.4)	6.1 (0.5)	3.8 (0.5)	6.5 (0.9)	6.6 (0.8)	4.5 (0.8)	6.5 (0.8)
UTrees-kMeans	6.0 (0.6)	5.8 (0.5)	6.3 (0.6)	6.1 (0.6)	4.1 (0.3)	4.0 (0.7)	2.9 (0.6)	3.8 (1)	6.0 (0.7)
UTrees-KDI	5.1 (0.5)	5.1 (0.5)	5.4 (0.6)	5.6 (0.5)	4.8 (0.3)	4.5 (0.9)	4.0 (0.5)	3.5 (1.2)	6.4 (0.7)
UTrees	3.8 (0.5)	3.2 (0.5)	3.8 (0.4)	3.8 (0.5)	5.0 (0.3)	2.7 (0.6)	2.9 (0.8)	3.5 (0.8)	5.8 (0.7)

observed data are shown in Table 4. UnmaskingTrees loses head-to-head to Forest-Flow, Forest-VP, and TabDDPM, but wins against the other methods.

Table 3: Tabular data generation with incomplete data (27 datasets, 3 experiments per dataset, 20% missing values), MissForest is used to impute missing data except in Forest-VP, Forest-Flow, and UnmaskingTrees; *averaged rank* over all datasets and experiments (standard-error). Overall best is **highlighted**; better of Forest-VP versus Forest-Flow versus ours is **boldface blue**.

	W_{train} ↓	W_{test} ↓	cov_{train} ↓	cov_{test} ↓	R_{fake}^2 ↓	$F1_{fake}$ ↓	$F1_{disc}$ ↓	P_{bias} ↓	cov_{rate} ↓
GaussianCopula	7.0 (0.3)	7.1 (0.2)	7.2 (0.3)	7.1 (0.3)	6.3 (0.4)	6.6 (0.3)	6.7 (0.4)	5.5 (1.0)	7.7 (0.6)
TVAE	5.2 (0.3)	4.9 (0.3)	5.7 (0.3)	5.8 (0.2)	6.0 (1.0)	5.8 (0.5)	5.8 (0.4)	8.0 (0.4)	6.2 (1.0)
CTGAN	8.3 (0.2)	8.4 (0.2)	8.4 (0.2)	8.3 (0.2)	8.3 (0.3)	8.4 (0.2)	6.5 (0.2)	4.8 (1.2)	7.1 (0.7)
CTABGAN	6.7 (0.4)	6.5 (0.4)	7.1 (0.3)	6.8 (0.3)	7.3 (0.6)	7.1 (0.4)	6.6 (0.3)	7.5 (1.0)	6.1 (0.6)
Stasy	5.9 (0.2)	6.1 (0.3)	5.3 (0.2)	5.1 (0.3)	5.8 (0.9)	4.4 (0.4)	5.3 (0.4)	3.7 (0.4)	4.6 (1.1)
TabDDPM	3.0 (0.7)	3.4 (0.7)	2.3 (0.5)	2.9 (0.6)	1.7 (0.3)	3.3 (0.6)	3.9 (0.6)	3.8 (1.2)	2.0 (0.5)
Forest-VP	3.7 (0.2)	3.2 (0.3)	3.9 (0.2)	3.8 (0.3)	3.2 (0.3)	2.3 (0.3)	4.2 (0.4)	4.2 (0.8)	4.5 (1.1)
Forest-Flow	3.0 (0.3)	2.6 (0.3)	2.6 (0.3)	2.7 (0.2)	3.0 (0.7)	3.7 (0.3)	5.0 (0.5)	3.8 (0.9)	3.2 (0.8)
UTrees	2.1 (0.2)	2.8 (0.3)	2.5 (0.2)	2.5 (0.2)	3.3 (0.8)	3.5 (0.5)	1.0 (0.0)	3.7 (0.9)	3.7 (1.0)

Table 4: Tabular data generation with complete data (27 datasets, 3 experiments per dataset); *averaged rank* over all datasets and experiments (standard-error). Overall best is **highlighted**; better of Forest-VP versus Forest-Flow versus ours is **boldface blue**.

	W_{train} ↓	W_{test} ↓	cov_{train} ↓	cov_{test} ↓	R_{fake}^2 ↓	$F1_{fake}$ ↓	$F1_{disc}$ ↓	P_{bias} ↓	Cov_{rate} ↓
GaussianCopula	7.1 (0.3)	7.2 (0.3)	7.3 (0.3)	7.4 (0.3)	6.2 (0.2)	6.4 (0.3)	7.0 (0.4)	6.5 (1.1)	7.5 (0.7)
TVAE	5.3 (0.2)	5.1 (0.2)	5.7 (0.2)	5.7 (0.2)	6.5 (0.7)	6.0 (0.5)	5.5 (0.3)	7.3 (0.6)	6.7 (0.6)
CTGAN	8.4 (0.1)	8.4 (0.2)	8.3 (0.2)	8.1 (0.2)	8.5 (0.2)	8.3 (0.2)	6.7 (0.3)	5.3 (1.1)	7.2 (0.5)
CTAB-GAN+	6.8 (0.3)	6.7 (0.3)	7.2 (0.3)	7.1 (0.3)	6.8 (0.4)	6.9 (0.4)	6.9 (0.3)	7.7 (0.8)	6.7 (0.8)
STaSy	6.1 (0.2)	6.3 (0.2)	5.3 (0.2)	5.4 (0.2)	6.0 (1.2)	5.1 (0.3)	6.1 (0.3)	4.5 (0.8)	4.2 (1.1)
TabDDPM	3.0 (0.7)	3.9 (0.6)	2.8 (0.5)	3.4 (0.5)	1.2 (0.2)	3.8 (0.6)	3.2 (0.4)	3.0 (0.9)	1.4 (0.2)
Forest-VP	3.2 (0.2)	2.8 (0.2)	3.6 (0.3)	3.3 (0.3)	2.8 (0.3)	2.2 (0.3)	4.3 (0.4)	3.2 (0.9)	3.5 (0.8)
Forest-Flow	1.9 (0.2)	1.5 (0.2)	1.7 (0.2)	1.8 (0.2)	2.3 (0.4)	2.4 (0.3)	4.3 (0.4)	2.8 (0.5)	2.7 (0.4)
UTrees	3.1 (0.1)	3.1 (0.2)	3.1 (0.2)	2.8 (0.2)	4.7 (0.3)	3.9 (0.3)	1.0 (0.0)	4.7 (0.7)	5.2 (0.9)

Raw scores, per-dataset results, and runtimes are provided in the Appendix.

3.3 EVALUATING BALTOBOT ON SYNTHETIC PROBABILISTIC PREDICTION CASE STUDIES

Wave dataset We compare our approach with Treeffuser (Beltran-Velez et al., 2024) on the “wave” synthetic dataset from Treeffuser (Beltran-Velez et al., 2024), which as shown in Figure 3 is nonlinear, multimodal, and heteroskedastic. On the raw probabilistic predictions in Figure 3(A), we see that BaltoBot and BaltoBoTabPFN are (by visual inspection) able to model the conditional distribution as well as Treeffuser. Yet this case study illustrates the two advantages of BaltoBot. First, in Figure 3(B) we show the runtime of the different methods: training, sampling, and total. To train on 5000 samples, Treeffuser took 1.1s and BaltoBot took 2.6s. But to generate 5000 samples, Treeffuser took 5.0s while BaltoBot took 0.72s, for $\sim 7\times$ speedup. Second, BaltoBot offers the ability to estimate a closed-form probability density function (pdf) of the predictive distribution as shown in Figure 3(C); in contrast, Treeffuser can only sample from the predictive distribution.

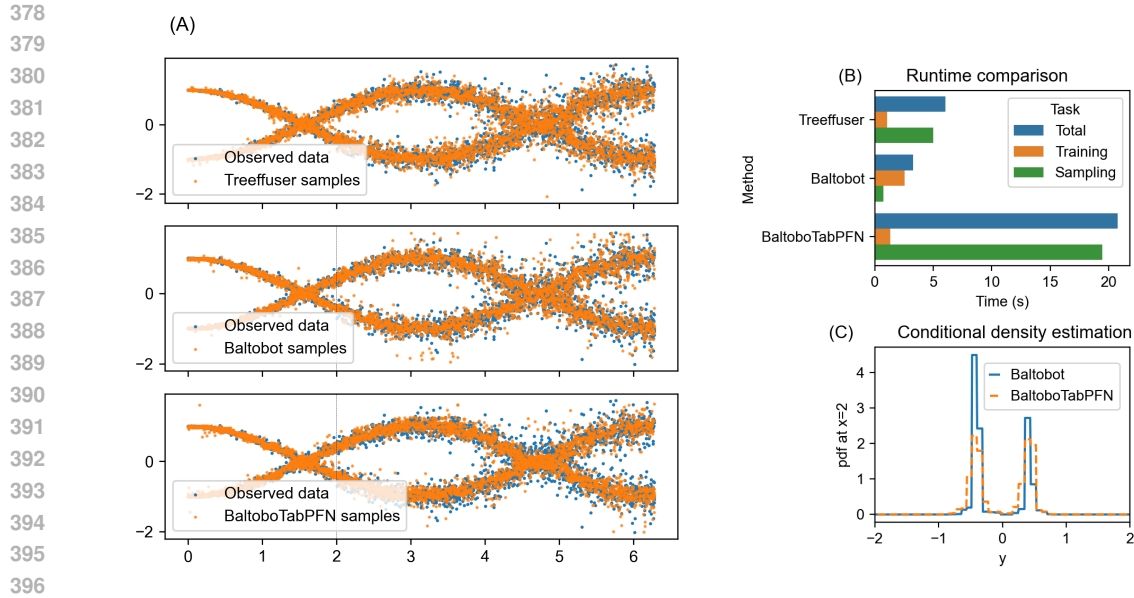


Figure 3: Comparison of Treeffuser and our approach on wave synthetic data with 5000 samples. (A) Probabilistic predictions for Treeffuser (top), BaltoBot (center), and BaltoBoTabPFN (bottom). (B) Runtime comparison for the different methods. (C) Estimated pdf from our methods at $X = 2$, depicted as the vertical dotted line in (A).

Poisson-distributed count data We generate 500 samples of $X_i \sim \text{Unif}[0, 3]$, $Y_i \sim \text{Poisson}(\lambda = \sqrt{X_i})$, and show probabilistic predictions for Y in Figure 4. Whereas Treeffuser generates a spurious negative-valued outlier and many non-integer Y samples, our approach automatically models the count-type distribution of the data.

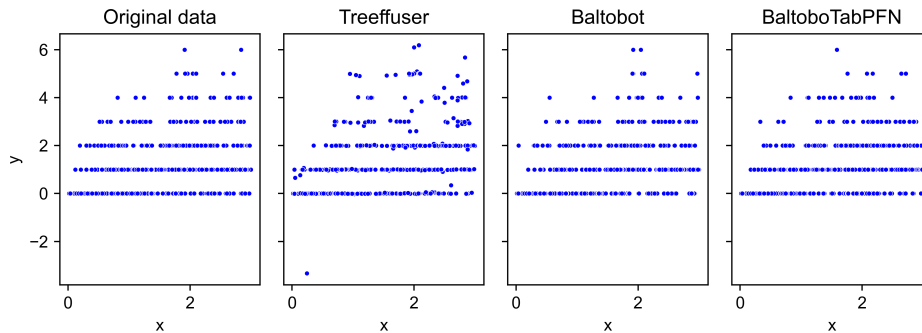


Figure 4: Comparison of Treeffuser, BaltoBot, and BaltoBoTabPFN on Poisson-distributed data. The input variable is on the x-axis, while probabilistic predictions are shown on the y-axis.

3.4 SALES FORECASTING WITH UNCERTAINTY

We employ the M5 sales forecasting Kaggle dataset (Makridakis & Howard, 2020) to compare BaltoBot with other probabilistic prediction methods. The dataset has five years of sales data from ten Walmart stores, and the task requires predicting the (heavy-tailed) number of units sold given a product’s attributes and previous sales. We use the exact same data preparation used for Treeffuser (Beltran-Velez et al., 2024) experiments, which yields 1k products, 120k training samples, and 10k test samples. As in the Treeffuser evaluation (Beltran-Velez et al., 2024), we evaluate probabilistic predictions with the continuous ranked probability score (CRPS), and evaluate the conditional mean predictions with the mean absolute error (MAE) and root mean-squared error (RMSE).

Table 5: Sales forecasting evaluation on M5 dataset. We **highlight** the best 2 methods for each metric. The best of Treeffuser versus ours (with tuning) is **boldface blue**; the best of Treeffuser versus ours (without tuning) is **boldface brown**.

Method	CRPS $\times 10^{-1}(\downarrow)$	RMSE $\times 10^0(\downarrow)$	MAE $\times 10^0(\downarrow)$
Deep Ensembles	7.05	2.03	0.97
IBUG	8.90	2.12	1.00
NGBoost Poisson	6.86	2.33	0.99
Quantile Regression Forests	7.11	2.88	1.01
Treeffuser	6.44	2.09	0.99
BaltoBot	6.44	2.07	0.98
Treeffuser (no tuning)	6.62	2.09	0.99
BaltoBot (no tuning)	6.69	2.19	0.98
BaltoBoTabPFN (no tuning)	6.66	2.06	0.97

For full comparability, we follow the Treeffuser evaluation setup (Beltran-Velez et al., 2024) and evaluate CRPS by generating 100 samples from our estimators’ $p(y|\mathbf{X})$ for each \mathbf{X} in the testset; and for MAE and RMSE, we estimate the conditional means $\mathbb{E}[y|\mathbf{X}]$ using 50 samples. For comparability, for this (and only this) dataset, we also evaluate BaltoBot with hyperparameter tuning, using the same setup used for all other methods (10 folds, each with 80%-20% train-validation split, and 25 Bayesian optimization iterations).² We also compare Treeffuser, BaltoBot, and BaltoBoTabPFN when run without hyperparameter tuning.

We report results in Table 5. In addition to ours’ and Treeffuser, we report results for Deep Ensembles (Lakshminarayanan et al., 2017), IBUG (Brophy & Lowd, 2022), NGBoost Poisson (Duan et al., 2020), and Quantile Regression Forests (Meinshausen & Ridgeway, 2006). For methods other than our own, we report the metrics provided in Table 2 of (Beltran-Velez et al., 2024). Overall, our proposed methods outperform previous methods at combining excellent performance on both conditional distribution prediction and conditional mean prediction. Treeffuser and BaltoBot (both with tuning) tie for first-place according to CRPS, yet BaltoBot outperforms Treeffuser on RMSE and MAE. The winners on conditional mean metrics (RMSE and MAE) are Deep Ensembles and BaltoBoTabPFN, yet BaltoBoTabPFN (no tuning) strongly outperforms Deep Ensembles on CRPS.

4 LIMITATIONS

While UnmaskingTrees is *overall* state-of-the-art on the tabular imputation benchmark, MissForest still outperformed on the metrics based on Wasserstein distance to train and test dataset distributions. And Forest-Flow still won on vanilla generation benchmark (without any missingness). It remains to be seen whether a single method can be developed which wins on all scenarios and metrics. While BaltoBoTabPFN performed well on probabilistic prediction tasks, when used as a subroutine in UnmaskingTabPFN, it is very slow and experienced out-of-memory errors on the (Jolicoeur-Martineau et al., 2024b) benchmark on our machine. Further improvements either to it, or to how it is employed, are needed to make it practical for all but the smallest datasets.

5 DISCUSSION AND RELATED WORK

Diffusion modeling has recently gained popularity in tabular ML (Zheng & Charoenphakdee, 2022; Jolicoeur-Martineau et al., 2024b; Beltran-Velez et al., 2024; Kotelnikov et al., 2023). Our proposed approach is an instance of the autoregressive discrete diffusion framework (Hoogeboom et al., 2021), instances of which have shown success in a variety of tasks (Yang, 2019; Austin et al., 2021; Kitouni et al., 2024; Jolicoeur-Martineau et al., 2024a). Yet our results call into question whether diffusion is beneficial for tabular conditional generation, or whether autoregression is sufficient for our setting.

²We optimize over the following XGBoost hyperparameter spaces: `learning_rate` \in `log-uniform(0.05, 0.5)`, `max_leaves` \in `{0, 25, 50}`, and `subsample` \in `log-uniform(0.3, 1)`.

486 It has been observed that diffusion is autoregression in frequency space, progressing from low
487 frequencies to high frequencies, which makes it a good match for image data with its power law
488 spectra (Rissanen et al., 2022; Dieleman, 2024; Stewart, 2024). In tabular datasets without this
489 phenomena, we would expect diffusion modeling to be less advantageous.

490 Why is ForestDiffusion better at vanilla generative modeling, while UnmaskingTrees is better on
491 missing data problems? We offer two speculative explanations. First, imputation is a conditional
492 modeling scenario, except that you do not know the partition of the features into input features
493 and output features *a priori*. One could address imputation by learning all possible 2^D conditional
494 distributions, but this is impractical for large D , so one would prefer to learn a single joint distribution.
495 Both autoregression and diffusion are ways of learning a joint distribution; because autoregression
496 does so by learning conditional distributions, it is more suited to the conditional modeling imputation
497 setting. Second, for missing data, diffusion has a train-inference gap: during training, observed
498 features begin the reverse process from $\mathcal{N}(0, 1)$; during inference for imputation, observed features
499 begin the reverse process at their actual values. On the other hand, the advantages of diffusion
500 modeling give it superiority when these problems can be avoided.

501 Despite their strong outperformance on other modalities, deep learning approaches have laboured
502 against gradient-boosted decision trees on tabular data (Shwartz-Ziv & Armon, 2022; Jolicoeur-
503 Martineau et al., 2024b). Previous work (Breejen et al., 2024) suggests that tabular data requires
504 an inductive prior that favors sharpness rather than smoothness, showing that TabPFN (Hollmann
505 et al., 2022) (the leading deep learning tabular classification method) can be further improved with
506 synthetic data generated from random forests. We anticipate that our XGBoost classifiers may be
507 swapped out for a future variant of TabPFN that learns sharper boundaries and handles missingness.

508 We also note that MissForest (Stekhoven & Bühlmann, 2012), hailing from statistical literature on
509 multiple imputation, has yet to be completely dethroned. Future progress in tabular conditional
510 generation may require going back to the well of this traditional literature. As one example, we
511 observe that MissForest exploits feature missingness fraction information, but we are not aware of any
512 “machine learning” approaches which do so. The statistical literature has also previously explored the
513 value of conditional modeling for joint modeling (Gelman & Raghunathan, 2001; Liu et al., 2014;
514 Kropko et al., 2014). Indeed, our UnmaskingTrees approach, and all autoregressive modeling, is
515 presaged by the full-mechanism bootstrap (Efron, 1994).

516 Finally, we observe where randomness enters into our generation process compared to previous work.
517 Flow-matching (Liu et al., 2022; Albergo & Vanden-Eijnden, 2022; Lipman et al., 2022) (used in
518 Forest-Flow) injects randomness solely at the beginning of the reverse process via Gaussian sampling,
519 whereas diffusion modeling (Sohl-Dickstein et al., 2015; Song & Ermon, 2019) (used in Forest-VP)
520 injects randomness both at the beginning and during the reverse process. In contrast, because our
521 method starts with a fully-masked sample, it injects randomness gradually during the generation
522 process. First, we randomly generate the order over features for unmasking. Second, we do not
523 “greedily decode” to the most likely leaf in the meta-tree, but instead sample according to predicted
524 probabilities. Third, for continuous features, having sampled a particular meta-tree leaf bin, we
525 sample from within the bin, treating it as a uniform distribution.

526 6 CONCLUSIONS

527
528 We proposed tree-based autoregressive modeling of tabular data, especially for data with missingness.
529 For the subproblem of conditional probabilistic prediction of individual variables, we presented a
530 hierarchical partitioning method with benefits over vanilla quantization and diffusion-based proba-
531 bilistic prediction. We then considered each of these as meta-algorithms that enable pure in-context
532 learning-based modeling using TabPFN as base classifier. We showed SotA results for imputation
533 and for generation given data with missingness, and on probabilistic prediction for sales forecasting.
534

535 7 REPRODUCIBILITY STATEMENT

536
537 All our code is in an anonymized public Github repo. We evaluate on public real datasets, using
538 experimental setups released by previous works; or on synthetic data, using scripts in our repo.
539

REFERENCES

- 540
541
542 Michael S Albergo and Eric Vanden-Eijnden. Building normalizing flows with stochastic interpolants.
543 *arXiv preprint arXiv:2209.15571*, 2022.
- 544 Jacob Austin, Daniel D Johnson, Jonathan Ho, Daniel Tarlow, and Rianne Van Den Berg. Structured
545 denoising diffusion models in discrete state-spaces. *Advances in Neural Information Processing*
546 *Systems*, 34:17981–17993, 2021.
- 547 Nicolas Beltran-Velez, Alessandro Antonio Grande, Achille Nazaret, Alp Kucukelbir, and David Blei.
548 Treeffuser: Probabilistic predictions via conditional diffusions with gradient-boosted trees. *arXiv*
549 *preprint arXiv:2406.07658*, 2024.
- 551 Felix den Breejen, Sangmin Bae, Stephen Cha, and Se-Young Yun. Why in-context learning
552 transformers are tabular data classifiers. *arXiv preprint arXiv:2405.13396*, 2024.
- 553 Leo Breiman. Random forests. *Machine learning*, 45:5–32, 2001.
- 554
555 Jonathan Brophy and Daniel Lowd. Instance-based uncertainty estimation for gradient-boosted
556 regression trees. *Advances in Neural Information Processing Systems*, 35:11145–11159, 2022.
- 557 Samuel F Buck. A method of estimation of missing values in multivariate data suitable for use with
558 an electronic computer. *Journal of the Royal Statistical Society: Series B (Methodological)*, 22(2):
559 302–306, 1960.
- 560 Rodrigo Castellon, Achintya Gopal, Brian Bloniarz, and David Rosenberg. Dp-tbart: A transformer-
561 based autoregressive model for differentially private tabular data generation. *arXiv preprint*
562 *arXiv:2307.10430*, 2023.
- 563
564 Tianqi Chen and Carlos Guestrin. Xgboost: A scalable tree boosting system. In *Proceedings of the*
565 *22nd acm sigkdd international conference on knowledge discovery and data mining*, pp. 785–794,
566 2016.
- 567 Sander Dieleman. Diffusion is spectral autoregression, 2024. URL [https://sander.ai/2024/](https://sander.ai/2024/09/02/spectral-autoregression.html)
568 [09/02/spectral-autoregression.html](https://sander.ai/2024/09/02/spectral-autoregression.html).
- 569
570 Tony Duan, Avati Anand, Daisy Yi Ding, Khanh K Thai, Sanjay Basu, Andrew Ng, and Alejandro
571 Schuler. Ngboost: Natural gradient boosting for probabilistic prediction. In *International*
572 *conference on machine learning*, pp. 2690–2700. PMLR, 2020.
- 573
574 Bradley Efron. Missing data, imputation, and the bootstrap. *Journal of the American Statistical*
575 *Association*, 89(426):463–475, 1994.
- 576 Ronald A Fisher. The use of multiple measurements in taxonomic problems. *Annals of eugenics*, 7
577 (2):179–188, 1936.
- 578 Andrew Gelman and Trivellore E Raghunathan. Using conditional distributions for missing-data
579 imputation. *Statistical Science*, 15:268–69, 2001.
- 580
581 Manbir Gulati and Paul Roysdon. Tabmt: Generating tabular data with masked transformers.
582 *Advances in Neural Information Processing Systems*, 36, 2024.
- 583
584 Trevor Hastie, Rahul Mazumder, Jason D Lee, and Reza Zadeh. Matrix completion and low-rank svd
585 via fast alternating least squares. *The Journal of Machine Learning Research*, 16(1):3367–3402,
586 2015.
- 587 David P Hofmeyr. Fast exact evaluation of univariate kernel sums. *IEEE transactions on pattern*
588 *analysis and machine intelligence*, 43(2):447–458, 2019.
- 589
590 Noah Hollmann, Samuel Müller, Katharina Eggenberger, and Frank Hutter. Tabpfn: A transformer
591 that solves small tabular classification problems in a second. *arXiv preprint arXiv:2207.01848*,
592 2022.
- 593 Emiel Hoogetboom, Alexey A Gritsenko, Jasmijn Bastings, Ben Poole, Rianne van den Berg, and
Tim Salimans. Autoregressive diffusion models. *arXiv preprint arXiv:2110.02037*, 2021.

- 594 Harry Joe. *Dependence modeling with copulas*. CRC press, 2014.
- 595
- 596 Alexia Jolicoeur-Martineau, Aristide Baratin, Kisoo Kwon, Boris Knyazev, and Yan Zhang. Any-
597 property-conditional molecule generation with self-criticism using spanning trees. *arXiv preprint*
598 *arXiv:2407.09357*, 2024a.
- 599 Alexia Jolicoeur-Martineau, Kilian Fatras, and Tal Kachman. Generating and imputing tabular data
600 via diffusion and flow-based gradient-boosted trees. In *International Conference on Artificial*
601 *Intelligence and Statistics*, pp. 1288–1296. PMLR, 2024b. URL [https://github.com/](https://github.com/SamsungSAILMontreal/ForestDiffusion)
602 [SamsungSAILMontreal/ForestDiffusion](https://github.com/SamsungSAILMontreal/ForestDiffusion).
- 603
- 604 Jayoung Kim, Chaejeong Lee, and Noseong Park. Stasy: Score-based tabular data synthesis. *arXiv*
605 *preprint arXiv:2210.04018*, 2022.
- 606 Ouail Kitouni, Niklas Nolte, James Hensman, and Bhaskar Mitra. Disk: A diffusion model for
607 structured knowledge. *arXiv preprint arXiv:2312.05253*, 2023.
- 608
- 609 Ouail Kitouni, Niklas Nolte, Diane Bouchacourt, Adina Williams, Mike Rabbat, and Mark Ibrahim.
610 The factorization curse: Which tokens you predict underlie the reversal curse and more. *arXiv*
611 *preprint arXiv:2406.05183*, 2024.
- 612 Akim Kotelnikov, Dmitry Baranchuk, Ivan Rubachev, and Artem Babenko. Tabddpm: Modelling
613 tabular data with diffusion models. In *International Conference on Machine Learning*, pp. 17564–
614 17579. PMLR, 2023.
- 615 Jonathan Kropko, Ben Goodrich, Andrew Gelman, and Jennifer Hill. Multiple imputation for
616 continuous and categorical data: comparing joint multivariate normal and conditional approaches.
617 *Political Analysis*, 22(4), 2014.
- 618
- 619 Balaji Lakshminarayanan, Alexander Pritzel, and Charles Blundell. Simple and scalable predictive
620 uncertainty estimation using deep ensembles. *Advances in neural information processing systems*,
621 30, 2017.
- 622 Quoc V Le, Tim Sears, and Alexander J Smola. Nonparametric quantile regression. Technical report,
623 Technical report, National ICT Australia, June 2005. Available at <http://sml...>, 2005.
- 624
- 625 Xiaotian Li, Shuzhe Wang, Yi Zhao, Jakob Verbeek, and Juho Kannala. Hierarchical scene coordinate
626 classification and regression for visual localization. *Proceedings of the IEEE/CVF Conference on*
627 *Computer Vision and Pattern Recognition*, pp. 11983–11992, 2020.
- 628
- 629 Yaron Lipman, Ricky TQ Chen, Heli Ben-Hamu, Maximilian Nickel, and Matt Le. Flow matching
630 for generative modeling. *arXiv preprint arXiv:2210.02747*, 2022.
- 631
- 632 Jingchen Liu, Andrew Gelman, Jennifer Hill, Yu-Sung Su, and Jonathan Kropko. On the stationary
633 distribution of iterative imputations. *Biometrika*, 101(1):155–173, 2014.
- 634
- 635 Xingchao Liu, Chengyue Gong, and Qiang Liu. Flow straight and fast: Learning to generate and
636 transfer data with rectified flow. *arXiv preprint arXiv:2209.03003*, 2022.
- 637
- 638 Stuart Lloyd. Least squares quantization in pcm. *IEEE transactions on information theory*, 28(2):
639 129–137, 1982.
- 640
- 641 Andreas Lugmayr, Martin Danelljan, Andres Romero, Fisher Yu, Radu Timofte, and Luc Van Gool.
642 Repaint: Inpainting using denoising diffusion probabilistic models. In *Proceedings of the*
643 *IEEE/CVF Conference on Computer Vision and Pattern Recognition (CVPR)*, pp. 11461–11471,
644 June 2022.
- 645
- 646 Junwei Ma, Apoorv Dankar, George Stein, Guangwei Yu, and Anthony Caterini. Tabpfgn–tabular
647 data generation with tabpfn. *arXiv preprint arXiv:2406.05216*, 2024.
- 648
- 649 Spyros Makridakis and Addison Howard. M5 forecasting - accuracy, 2020. URL [https://](https://kaggle.com/competitions/m5-forecasting-accuracy)
650 kaggle.com/competitions/m5-forecasting-accuracy.
- 651
- 652 Alexander März. Xgboostlss—an extension of xgboost to probabilistic forecasting. *arXiv preprint*
653 *arXiv:1907.03178*, 2019.

- 648 Calvin McCarter. The kernel density integral transformation. *Transactions on Machine Learning*
649 *Research*, 2023. ISSN 2835-8856.
- 650
651 Duncan McElfresh, Sujay Khandagale, Jonathan Valverde, Vishak Prasad C, Ganesh Ramakrishnan,
652 Micah Goldblum, and Colin White. When do neural nets outperform boosted trees on tabular data?
653 *Advances in Neural Information Processing Systems*, 36, 2024.
- 654 Nicolai Meinshausen and Greg Ridgeway. Quantile regression forests. *Journal of machine learning*
655 *research*, 7(6), 2006.
- 656 Boris Muzellec, Julie Josse, Claire Boyer, and Marco Cuturi. Missing data imputation using optimal
657 transport. In *International Conference on Machine Learning*, pp. 7130–7140. PMLR, 2020.
- 658
659 Severi Rissanen, Markus Heinonen, and Arno Solin. Generative modelling with inverse heat dissipa-
660 tion. *arXiv preprint arXiv:2206.13397*, 2022.
- 661 Ravid Shwartz-Ziv and Amitai Armon. Tabular data: Deep learning is not all you need. *Information*
662 *Fusion*, 81:84–90, 2022.
- 663
664 Jascha Sohl-Dickstein, Eric Weiss, Niru Maheswaranathan, and Surya Ganguli. Deep unsupervised
665 learning using nonequilibrium thermodynamics. In *International conference on machine learning*,
666 pp. 2256–2265. PMLR, 2015.
- 667 Yang Song and Stefano Ermon. Generative modeling by estimating gradients of the data distribution.
668 *Advances in neural information processing systems*, 32, 2019.
- 669
670 Olivier Sprangers, Sebastian Schelter, and Maarten de Rijke. Probabilistic gradient boosting machines
671 for large-scale probabilistic regression. In *Proceedings of the 27th ACM SIGKDD conference on*
672 *knowledge discovery & data mining*, pp. 1510–1520, 2021.
- 673 Daniel J Stekhoven and Peter Bühlmann. Missforest—non-parametric missing value imputation for
674 mixed-type data. *Bioinformatics*, 28(1):112–118, 2012.
- 675
676 Riley Stewart. transformers are kiki, diffusion is bouba, and language is pointier than images, 2024.
677 URL https://x.com/riley_stews/status/1827089629369266492.
- 678
679 Olga Troyanskaya, Michael Cantor, Gavin Sherlock, Pat Brown, Trevor Hastie, Robert Tibshirani,
680 David Botstein, and Russ B Altman. Missing value estimation methods for dna microarrays.
681 *Bioinformatics*, 17(6):520–525, 2001.
- 682
683 Stef Van Buuren, Hendriek C Boshuizen, and Dick L Knook. Multiple imputation of missing blood
684 pressure covariates in survival analysis. *Statistics in medicine*, 18(6):681–694, 1999.
- 685
686 A Vaswani. Attention is all you need. *Advances in Neural Information Processing Systems*, 2017.
- 687
688 Max Welling and Yee W Teh. Bayesian learning via stochastic gradient langevin dynamics. In
689 *Proceedings of the 28th international conference on machine learning (ICML-11)*, pp. 681–688.
690 Citeseer, 2011.
- 691
692 Samuel Von Wilson, Bogdan Cebere, James Myatt, and Samuel Wilson. AnotherSamWil-
693 son/miceforest: Release for Zenodo DOI, December 2022. URL <https://doi.org/10.5281/zenodo.7428632>.
- 694
695 Lei Xu, Maria Skoularidou, Alfredo Cuesta-Infante, and Kalyan Veeramachaneni. Modeling tabular
696 data using conditional gan. *Advances in neural information processing systems*, 32, 2019.
- 697
698 Z Yang. Xlnet: Generalized autoregressive pretraining for language understanding. *arXiv preprint*
699 *arXiv:1906.08237*, 2019.
- 700
701 Jinsung Yoon, James Jordon, and Mihaela Schaar. Gain: Missing data imputation using generative
adversarial nets. In *International conference on machine learning*, pp. 5689–5698. PMLR, 2018.
- Zilong Zhao, Aditya Kumar, Robert Birke, and Lydia Y Chen. Ctab-gan: Effective table data
synthesizing. In *Asian Conference on Machine Learning*, pp. 97–112. PMLR, 2021.
- Shuhan Zheng and Nontawat Charoenphakdee. Diffusion models for missing value imputation in
tabular data. *arXiv preprint arXiv:2210.17128*, 2022.

A ALGORITHMIC DESCRIPTIONS OF UNMASKINGTREES AND BALTOBOT

The training algorithm for UnmaskingTrees is given in 1. The training and inference algorithms for BaltoBot are given in 2 and 3, respectively.

Algorithm 1 Unmasking Trees training

Require: dataset $\mathbf{X} \in \mathbb{R}^{N \times D}$; duplication factor K .

- 1: {# Build self-supervised training set}
- 2: Set $\mathbf{X}_{\text{train}} = \emptyset, \mathbf{Y}_{\text{train}} = \emptyset$.
- 3: **for** $k = 1, \dots, K$ **do**
- 4: **for** $n = 1, \dots, N$ **do**
- 5: Draw random permutation σ from $\mathcal{U}(G_D)$
- 6: Set $\mathbf{x} := \mathbf{X}_{n,:}$; and $\mathbf{y} := \mathbf{X}_{n,:}$.
- 7: **for** $d = 1, \dots, D$ **do**
- 8: Mask random element $x_{\sigma(d)} := [\text{MASK}]$.
- 9: Append $\mathbf{X}_{\text{train}} := \mathbf{X}_{\text{train}} \cup \{\mathbf{x}\}, \mathbf{Y}_{\text{train}} := \mathbf{Y}_{\text{train}} \cup \{\mathbf{y}\}$
- 10: **end for**
- 11: **end for**
- 12: **end for**
- 13: {# Train conditional generation models}
- 14: **for** $d = 1, \dots, D$ **do**
- 15: **if** feature d in \mathbf{X} is a continuous feature **then**
- 16: Run BaltoBot with $([\mathbf{X}_{\text{train}}]_{:,j \neq d}, [\mathbf{Y}_{\text{train}}]_{:,d})$.
- 17: **else**
- 18: Train XGBClassifier on $([\mathbf{X}_{\text{train}}]_{:,j \neq d}, [\mathbf{Y}_{\text{train}}]_{:,d})$.
- 19: **end if**
- 20: **end for**

Algorithm 2 BaltoBot training

Require: dataset $(\mathbf{X} \in \mathbb{R}^{N \times D}, \mathbf{y} \in \mathbb{R}^N)$; BaltoBot meta-tree height H ;

- 1: **if** $H = 0$ **or** $\text{unique}(\mathbf{y}) = C$ for some constant C **then**
- 2: Save bounds $:= (\min(\mathbf{y}), \max(\mathbf{y}))$.
- 3: **else**
- 4: Obtain split point p from KDI quantization on \mathbf{y} .
- 5: Train XGBoost binary classifier on $(\mathbf{X}, \mathbf{1}\{\mathbf{y} \leq p\})$.
- 6: Train “left-child” BaltoBot on $\{(\mathbf{X}^{(i)}, \mathbf{y}^{(i)}) \in (\mathbf{X}, \mathbf{y}) | \mathbf{y}^{(i)} \leq p\}$, with height $H - 1$.
- 7: Train “right-child” BaltoBot on $\{(\mathbf{X}^{(i)}, \mathbf{y}^{(i)}) \in (\mathbf{X}, \mathbf{y}) | \mathbf{y}^{(i)} > p\}$, with height $H - 1$.
- 8: **end if**

Algorithm 3 BaltoBot inference

Require: input query $\mathbf{x} \in \mathbb{R}^D$; trained BaltoBot model.

- 1: **if** bounds is defined **then**
- 2: Sample uniformly from $U(\text{bounds})$.
- 3: Return.
- 4: **else**
- 5: Obtain *prediction* from XGBoost binary classifier.
- 6: **if** *prediction* = left-child **then**
- 7: Run inference on “left-child” BaltoBot with input query \mathbf{x} .
- 8: **else if** *prediction* = right-child **then**
- 9: Run inference on “right-child” BaltoBot with input query \mathbf{x} .
- 10: **end if**
- 11: **end if**

B ABLATION EXPERIMENT WITH IMPUTATION - RAW SCORES

Raw scores (shown in Table 6) demonstrate that UnmaskingTrees on its own improves upon Forest-VP's diffusion approach. We also see that KDI quantization (with 20 bins) contributes to improvement beyond k-Means (also 20 bins), and that BaltoBot yields even further improvement.

Table 6: Raw scores from ablation study for tabular data imputation (27 datasets, 3 experiments per dataset, 10 imputations per experiment) with 20% missing values. Shown are raw scores - mean (standard-error). Overall best is **highlighted**; better of Forest-VP versus ours is **boldface blue**. See Table 1 for column meanings.

	MinMAE ↓	AvgMAE ↓	W_{train} ↓	W_{test} ↓	MAD ↑	R_{imp}^2 ↑	$F1_{imp}$ ↑	P_{bias} ↓	$Covrate$ ↑
KNN	0.16 (0.03)	0.16 (0.03)	0.42 (0.08)	1.89 (0.49)	0 (0)	0.59 (0.09)	0.75 (0.04)	1.27 (0.25)	0.4 (0.11)
ICE	0.1 (0.01)	0.21 (0.03)	0.52 (0.09)	1.99 (0.49)	0.69 (0.1)	0.59 (0.09)	0.74 (0.04)	1.05 (0.29)	0.39 (0.09)
MICE-Forest	0.08 (0.02)	0.13 (0.03)	0.34 (0.07)	1.86 (0.48)	0.29 (0.08)	0.61 (0.1)	0.76 (0.04)	0.61 (0.2)	0.75 (0.11)
MissForest	0.1 (0.03)	0.12 (0.03)	0.32 (0.07)	1.85 (0.48)	0.1 (0.03)	0.61 (0.1)	0.76 (0.04)	0.62 (0.22)	0.79 (0.08)
Softimpute	0.22 (0.03)	0.22 (0.03)	0.53 (0.07)	1.99 (0.48)	0 (0)	0.58 (0.09)	0.74 (0.04)	1.18 (0.34)	0.31 (0.09)
OT	0.14 (0.02)	0.19 (0.03)	0.56 (0.1)	1.98 (0.49)	0.28 (0.05)	0.59 (0.1)	0.75 (0.04)	1.09 (0.27)	0.39 (0.12)
GAIN	0.16 (0.03)	0.17 (0.03)	0.49 (0.11)	1.95 (0.51)	0.01 (0)	0.6 (0.1)	0.75 (0.04)	1.04 (0.25)	0.54 (0.12)
Forest-VP	0.14 (0.04)	0.17 (0.03)	0.55 (0.13)	1.96 (0.5)	0.25 (0.03)	0.61 (0.1)	0.74 (0.04)	0.81 (0.25)	0.57 (0.14)
UTrees-kMeans	0.1 (0.02)	0.15 (0.03)	0.43 (0.09)	1.9 (0.5)	0.28 (0.06)	0.61 (0.1)	0.76 (0.04)	0.63 (0.21)	0.72 (0.13)
UTrees-KDI	0.1 (0.02)	0.14 (0.03)	0.42 (0.09)	1.89 (0.49)	0.27 (0.06)	0.61 (0.1)	0.76 (0.04)	0.68 (0.24)	0.68 (0.14)
UTrees	0.08 (0.02)	0.14 (0.03)	0.37 (0.08)	1.87 (0.48)	0.27 (0.07)	0.61 (0.1)	0.76 (0.04)	0.55 (0.19)	0.71 (0.13)
Oracle	0 (0)	0 (0)	0 (0)	1.87 (0.49)	0 (0)	0.64 (0.09)	0.78 (0.04)	0 (0)	1 (0)

C FULL DATASET-LEVEL RESULTS

Full imputation results are in Table 7. Full generation results are in Table 8. Timing results are in Table 9, and depicted in Figure 5. Our method is relatively efficient at both imputation and generation. The datasets on which we are slowest for imputation are Libras (1976 seconds) and Bean (1929 seconds), on our ancient 2015 iMac with 16Gb RAM. On Libras, ForestVP imputation took 12439 seconds (without RePaint) and 14715 seconds (with RePaint); on Bean, ForestVP took 898 seconds (without RePaint) and 1318 seconds (with RePaint), on their cluster of 10-20 CPUs with 64-256Gb of RAM. The datasets on which we are slowest for generation are also Libras (2987 seconds) and Bean (4346 seconds). On Libras, ForestFlow generation took 9481 seconds and ForestVP took 9042 seconds; on Bean, ForestFlow took 869 seconds and ForestVP took 947 seconds, once again on their much more powerful computing cluster.

Table 7: Full imputation results for UnmaskingTrees on benchmark of 27 datasets.

Dataset	MinMAE ↓	AvgMAE ↓	P_{bias} ↓	$Covrate$ ↑	W_{train} ↓	W_{test} ↓	Variance ↑	MAD (mean) ↑	MAD (median) ↑	R^2 ↑	$F1$ ↑
iris	6.00e-02	8.91e-02	0.00e+00	0.00e+00	6.62e-02	2.40e-01	2.65e-03	1.48e-01	1.22e-01	0.00e+00	9.53e-01
wine	9.48e-02	1.31e-01	0.00e+00	0.00e+00	3.54e-01	1.44e+00	5.64e-03	2.37e-01	1.99e-01	0.00e+00	9.37e-01
parkinsons	4.69e-02	6.52e-02	0.00e+00	0.00e+00	2.94e-01	1.71e+00	2.73e-03	1.23e-01	1.03e-01	0.00e+00	8.30e-01
climate model crashes	2.38e-01	3.38e-01	0.00e+00	0.00e+00	1.22e+00	3.87e+00	4.38e-02	7.94e-01	6.88e-01	0.00e+00	7.08e-01
concrete compression	2.33e-02	5.19e-02	1.17e+02	2.44e-01	7.95e-02	5.05e-01	5.61e-03	1.59e-01	1.30e-01	7.55e-01	0.00e+00
yacht hydrodynamics	2.72e-02	6.53e-02	8.78e+01	9.62e-01	6.46e-02	5.11e-01	1.22e-02	1.90e-01	1.45e-01	8.96e-01	0.00e+00
airfoil self noise	2.42e-02	6.64e-02	3.37e+00	1.00e+00	4.60e-02	2.50e-01	1.25e-02	2.29e-01	1.84e-01	7.24e-01	0.00e+00
connectionist bench sonar	9.86e-02	1.18e-01	0.00e+00	0.00e+00	1.43e+00	8.51e+00	5.14e-03	2.22e-01	1.88e-01	0.00e+00	7.99e-01
ionosphere	8.52e-02	1.18e-01	0.00e+00	0.00e+00	7.82e-01	4.44e+00	1.47e-02	2.54e-01	2.02e-01	0.00e+00	9.10e-01
qsar biodegradation	1.53e-02	2.34e-02	0.00e+00	0.00e+00	1.92e-01	1.39e+00	1.25e-03	5.35e-02	4.36e-02	0.00e+00	8.49e-01
seeds	5.36e-02	8.45e-02	0.00e+00	0.00e+00	1.22e-01	4.78e-01	3.37e-03	1.74e-01	1.48e-01	0.00e+00	8.83e-01
glass	4.96e-02	7.59e-02	0.00e+00	0.00e+00	1.40e-01	6.42e-01	5.09e-03	1.44e-01	1.17e-01	0.00e+00	5.43e-01
ecoli	5.15e-02	8.00e-02	0.00e+00	0.00e+00	1.09e-01	4.04e-01	3.60e-03	1.54e-01	1.30e-01	0.00e+00	6.83e-01
yeast	4.38e-02	7.40e-02	0.00e+00	0.00e+00	1.07e-01	3.19e-01	3.58e-03	1.73e-01	1.50e-01	0.00e+00	4.44e-01
libras	3.06e-02	3.64e-02	0.00e+00	0.00e+00	6.57e-01	8.93e+00	8.11e-04	8.17e-02	7.06e-02	0.00e+00	5.69e-01
planning relax	8.41e-02	1.21e-01	0.00e+00	0.00e+00	3.06e-01	1.46e+00	5.57e-03	2.39e-01	2.03e-01	0.00e+00	4.52e-01
blood transfusion	3.44e-02	6.69e-02	0.00e+00	0.00e+00	3.21e-02	1.12e-01	4.80e-03	1.58e-01	1.32e-01	0.00e+00	5.87e-01
breast cancer diagnostic	3.96e-02	5.16e-02	0.00e+00	0.00e+00	3.10e-01	1.85e+00	1.21e-03	1.01e-01	8.73e-02	0.00e+00	9.59e-01
connectionist bench vowel	5.30e-02	9.39e-02	0.00e+00	0.00e+00	1.88e-01	7.25e-01	5.53e-03	2.48e-01	2.14e-01	0.00e+00	6.64e-01
concrete slump	1.25e-01	1.88e-01	4.76e+01	7.25e-01	2.64e-01	1.16e+00	1.48e-02	3.40e-01	2.75e-01	6.75e-01	0.00e+00
wine quality red	4.08e-02	7.16e-02	2.01e+01	1.00e+00	1.41e-01	5.17e-01	3.52e-03	1.83e-01	1.58e-01	3.06e-01	0.00e+00
wine quality white	3.41e-02	6.45e-02	7.74e+01	4.78e-01	1.40e-01	4.53e-01	3.36e-03	1.91e-01	1.68e-01	3.38e-01	0.00e+00
california	1.97e-02	4.97e-02	2.32e+01	5.93e-01	0.00e+00	0.00e+00	4.98e-03	1.58e-01	1.40e-01	6.55e-01	0.00e+00
bean	1.02e-02	2.06e-02	0.00e+00	0.00e+00	0.00e+00	0.00e+00	1.05e-03	6.42e-02	5.80e-02	0.00e+00	7.82e-01
tictactoe	2.96e-01	5.11e-01	0.00e+00	0.00e+00	7.76e-01	1.93e+00	2.45e-02	1.47e+00	1.13e+00	0.00e+00	8.23e-01
congress	1.73e-01	2.77e-01	0.00e+00	0.00e+00	8.03e-01	2.38e+00	9.76e-03	5.86e-01	4.33e-01	0.00e+00	9.33e-01
car	4.04e-01	6.85e-01	0.00e+00	0.00e+00	4.84e-01	1.07e+00	2.95e-02	2.06e+00	1.65e+00	0.00e+00	8.01e-01

Table 8: Full generation results for UnmaskingTrees on benchmark of 27 datasets.

Dataset	W_{train}	W_{test}	cov_{train}	cov_{test}	R_{fake}^2	$F1_{fake}$	$F1_{disc}$	P_{bias}	$Covrate$
iris	2.34e-01	3.41e-01	8.78e-01	9.16e-01	0.00e+00	9.25e-01	4.23e-01	0.00e+00	0.00e+00
wine	1.09e+00	1.53e+00	9.09e-01	9.37e-01	0.00e+00	9.15e-01	3.46e-01	0.00e+00	0.00e+00
parkinsons	1.34e+00	1.77e+00	7.48e-01	9.08e-01	0.00e+00	7.33e-01	3.56e-01	0.00e+00	0.00e+00
climate model crashes	3.26e+00	3.89e+00	8.96e-01	9.50e-01	0.00e+00	5.39e-01	2.81e-01	0.00e+00	0.00e+00
concrete compression	4.63e-01	6.21e-01	5.11e-01	8.16e-01	6.73e-01	0.00e+00	4.15e-01	1.50e+02	2.00e-01
yacht hydrodynamics	4.20e-01	6.36e-01	6.13e-01	7.89e-01	8.46e-01	0.00e+00	5.14e-01	1.42e+02	4.48e-01
airfoil self noise	1.93e-01	2.93e-01	6.39e-01	8.96e-01	6.09e-01	0.00e+00	4.65e-01	1.97e+01	4.78e-01
connectionist bench sonar	7.21e+00	8.96e+00	6.87e-01	8.89e-01	0.00e+00	7.20e-01	3.69e-01	0.00e+00	0.00e+00
ionosphere	3.84e+00	4.66e+00	6.11e-01	7.94e-01	0.00e+00	8.57e-01	4.22e-01	0.00e+00	0.00e+00
qsar biodegradation	1.34e+00	1.62e+00	4.81e-01	8.19e-01	0.00e+00	8.02e-01	4.44e-01	0.00e+00	0.00e+00
seeds	3.51e-01	5.48e-01	8.98e-01	9.63e-01	0.00e+00	8.69e-01	3.09e-01	0.00e+00	0.00e+00
glass	4.52e-01	7.12e-01	8.27e-01	9.35e-01	0.00e+00	4.41e-01	3.65e-01	0.00e+00	0.00e+00
ecoli	2.86e-01	4.38e-01	8.99e-01	9.58e-01	0.00e+00	6.16e-01	3.78e-01	0.00e+00	0.00e+00
yeast	2.44e-01	3.49e-01	8.54e-01	9.44e-01	0.00e+00	3.62e-01	4.32e-01	0.00e+00	0.00e+00
libras	1.01e+01	1.16e+01	4.65e-01	8.43e-01	0.00e+00	3.54e-01	3.44e-01	0.00e+00	0.00e+00
planning relax	1.02e+00	1.47e+00	9.22e-01	9.98e-01	0.00e+00	4.56e-01	3.07e-01	0.00e+00	0.00e+00
blood transfusion	1.00e-01	1.52e-01	9.62e-01	9.56e-01	0.00e+00	5.95e-01	4.07e-01	0.00e+00	0.00e+00
breast cancer diagnostic	1.55e+00	1.90e+00	7.94e-01	9.12e-01	0.00e+00	9.40e-01	3.43e-01	0.00e+00	0.00e+00
connectionist bench vowel	7.04e-01	8.87e-01	3.04e-01	8.34e-01	0.00e+00	5.75e-01	3.43e-01	0.00e+00	0.00e+00
concrete slump	6.24e-01	1.20e+00	8.71e-01	8.57e-01	5.34e-01	0.00e+00	3.52e-01	4.57e+01	5.75e-01
wine quality red	4.30e-01	5.40e-01	8.63e-01	9.67e-01	2.46e-01	0.00e+00	4.51e-01	5.14e+01	7.94e-01
wine quality white	4.23e-01	4.97e-01	8.26e-01	9.55e-01	2.52e-01	0.00e+00	4.46e-01	1.84e+02	2.83e-01
california	0.00e+00	0.00e+00	6.22e-01	9.03e-01	3.05e-01	0.00e+00	4.30e-01	1.75e+02	1.70e-01
bean	0.00e+00	0.00e+00	3.35e-01	7.53e-01	0.00e+00	8.16e-01	3.97e-01	0.00e+00	0.00e+00
tictactoe	9.44e-01	1.95e+00	8.23e-01	6.28e-01	0.00e+00	8.31e-01	2.74e-01	0.00e+00	0.00e+00
congress	1.38e+00	2.46e+00	9.11e-01	9.16e-01	0.00e+00	9.47e-01	2.87e-01	0.00e+00	0.00e+00
car	4.61e-01	1.05e+00	5.82e-01	5.20e-01	0.00e+00	7.99e-01	3.02e-01	0.00e+00	0.00e+00

Table 9: Runtime results for UnmaskingTrees on benchmark of 27 datasets.

Dataset	# Samples	# Features	Imputation time (s)	Generation time (s)
iris	150	4	5.31	10.72
wine	178	13	26.76	49.06
parkinsons	195	22	58.98	105.27
climate model crashes	540	18	103.73	207.70
concrete compression	1030	8	47.19	123.10
yacht hydrodynamics	308	6	8.89	22.36
airfoil self noise	1503	5	29.91	92.74
connectionist bench sonar	208	60	440.60	685.94
ionosphere	351	33	201.81	362.05
qsar biodegradation	1055	41	560.58	909.87
seeds	210	7	14.94	27.65
glass	214	9	17.12	33.78
ecoli	336	7	14.69	32.56
yeast	1484	8	62.96	150.93
libras	360	90	1975.78	2986.78
planning relax	182	12	25.25	46.18
blood transfusion	748	4	13.16	37.24
breast cancer diagnostic	569	30	279.33	495.71
connectionist bench vowel	990	10	79.85	179.48
concrete slump	103	7	9.74	16.49
wine quality red	1599	10	106.23	263.92
wine quality white	4898	11	357.68	890.90
california	20640	8	968.14	2754.75
bean	13611	16	1929.16	4345.50
tictactoe	958	9	25.85	51.77
congress	435	16	30.41	52.56
car	1728	6	30.18	60.38

864
865
866
867
868
869
870
871
872
873
874
875
876
877
878
879
880
881
882
883
884
885
886
887
888
889
890
891
892
893
894
895
896
897
898
899
900
901
902
903
904
905
906
907
908
909
910
911
912
913
914
915
916
917

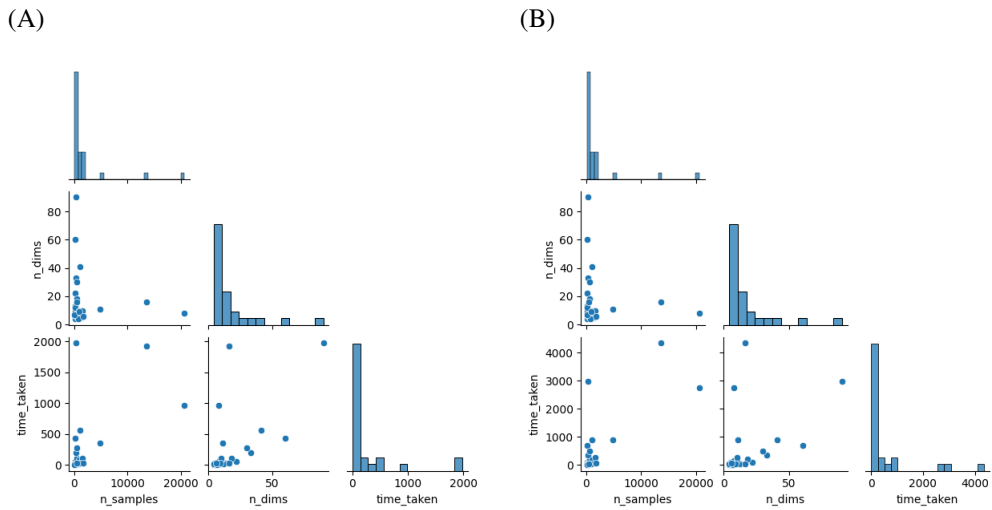


Figure 5: Runtime in seconds compared to number of features and number of samples, for imputation (A) and generation (B) tasks.